

Quantitative Analysis of Relative Tectonic Activities of Geothermal Areas of Lainea, South Konawe District, Southeast Sulawesi Province, Indonesia

La Hamimu^a, Suryawan Asfar^{b,*}, Arisona^b, L.O Ngkoimani^b, Silvara^b, Irawati^a, Al Rubaiyn^a

^a Department of Geophysics Engineering, Halu Oleo University, Kendari, 93232, Indonesia

^b Department of Geological Engineering, Halu Oleo University, Kendari, 93232, Indonesia

Corresponding author: *suryawan_tambang@uho.ac.id

Abstract— The tectonic activity that occurs in the Southeast Sulawesi Province causes this area to be traversed by many geological structures in the forms of faults trending Northwest-Southeast, and it is estimated that it is still active today. One evidence of the activity of these faults is the emergence of geothermal manifestations of Lainea. Therefore, this research was conducted to prove the level of tectonic activeness of an area as a part of mitigating potential natural disasters that might occur. This research activity aims to determine the level of tectonic activeness in the research area. So that from this purpose, the researcher uses the method, namely the quantitative geomorphic method, which includes morphotectonics analysis using the Digital Elevation Model data combined with direct observation of the type of lithology, geomorphological features, and geological structures that develop in the study area to produce a Relative Tectonic Activity Index. The results obtained from this study where the class of tectonic activity in the study area is divided into three tectonic activity classes, namely high tectonic activity classes in watersheds 4 and 7 with an area of $\pm 20.5 \text{ km}^2$, medium tectonic activity class in watershed 1, 5, 6, 8, 9 with an area of $\pm 40.9 \text{ km}^2$, and low tectonic activity class in watersheds 2 and 3 with an area of $\pm 12.8 \text{ km}^2$. Areas that have a high tectonic activity class have the potential for seismic hazards caused by the movement of geological structures found in the study area.

Keywords—Tectonics; watershed; morphotectonic; relative tectonic activity index (IATR).

Manuscript received 7 Dec. 2020; revised 27 Mar. 2021; accepted 13 Jun. 2021. Date of publication 31 Oct. 2022.
IJASEIT is licensed under a Creative Commons Attribution-Share Alike 4.0 International License.



I. INTRODUCTION

Based on the geographical aspect, Sulawesi Island is located in the central part of the Indonesia Archipelago [1], [2]. Meanwhile, based on the geological aspect, Sulawesi Island is located in the triple junction of the Indo-Australian, Eurasian and Pacific plates [3]–[6]. As a result, Sulawesi Island has a very high level of geological complexity on the earth's surface.

The tectonic activity that occurs has resulted in a variety of lithological types and the emergence of several faults/faults found in the Sulawesi region, namely: the Malino fault, Gorontalo fault, Palu-Koro fault, Parigi fault, Sapu fault, Bada fault, Poso fault, Balantak fault, Matano fault, Kendari fault, Lawanopo fault, Towuti fault [3], [7], some of these faults may be part of active faults which to this day continue to experience movement. An active fault is a fault that has experience displacements/movement and seismic activity in

the last 10.000 years [8]. The fracture that occurs in the rock has the potential to develop into a fault [9]. Apart from fault movement and seismic activity, active faults can also reconstruct a geothermal system, for example, is a non-volcanic manifestation of geothermal energy where the effect of fractures on the earth's surface allows hot fluids to rise to the surface and forming a pattern of distribution of geothermal manifestation points. Therefore, it can be assumed that with the presence of a geothermal system, it can be said that there are fault lines that have potential levels of activity in the area.

Research related to active faults is very important as part of efforts to mitigate so that it is easy to understand the potential for disasters in the area [10]. The characteristics of geomorphic features in an active fault area are very important to estimate the effect of tectonic movements along the fault and the current geological conditions; therefore, analyzing geomorphological parameters will help understand the current tectonic activity [11]. Assessment of the shape of the

landscape can be carried out from qualitative and quantitative (morphotectonic). The results of the assessment can produce the degree of tectonic activity that occurred in the past [12].

Several previous studies have conducted geomorphic index analysis to assess the level of tectonic activity, where this analysis uses Digital Elevation Model (DEM) data, satellite image maps, and field data [9], [12]–[18]. This research activity was carried out in the Southeast Sulawesi Arm area, where a geothermal manifestation phenomenon called Lainea geothermal system is precisely located in Lainea Village. This geothermal system is produced by the presence of southwest-northeast micro faults, namely the Boro-Boro Fault, Kaendi Fault, Landai Fault, Amowolo Fault, Lainea Fault, and Rumbalaka Fault where this fault is suspected. Also formed due to the implications that occurred when the tectonic process of Sulawesi Island was formed [19]. This research activity aims to determine the relative tectonic activity level in the Lainea geothermal area by using the relative tectonic activity index (IATR) so that it will be useful to understand the development of tectonic activity in that area.

Based on the regional geological conditions of the study area, several rock units are composed as follows [20]:

- Metamorphic rock units with the lithology types make up rock, phyllite, schist, and quartzite.
- Meta-limestone unit with a lithological type in the form of metamorphic limestone
- Meta-sandstone rock units with a lithological type are metamorphic sandstones with the insertion of quartzite.
- Non-carbonate sandstone units with a lithology type in the form of sandstones with black claystone inserts.
- The limestone-sandstones unit with the lithology type is in the form of sandstones containing Mollusca fossils.
- A conglomerate rock unit with a lithological type in the form of a conglomerate having a boulder-crust grain size.
- Alluvium rock units are composed of blocks, sand, gravel, gravel, and clay. As shown in Fig. 1

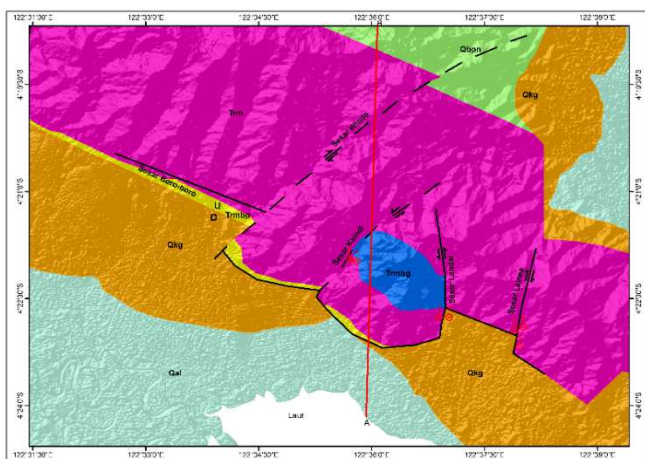


Fig. 1 A regional geological map is composed of several lithology types, namely metamorphic rock units, meta-limestone rock units, meta-sandstone rock units, non-carbonate sandstone units, limestone-limestone units, and conglomerate and alluvium rock units [20].

The geological structure condition where there are 3 groups of faults divided based on their direction:

- Fault's trending northwest-southeast includes the Boro-Boro fault, Andinete fault, Aonope fault, Sibingguru fault, Putemata fault.
- Fault's trending southwest-northeast includes the Wolasi fault, Anggowila fault, Hariri fault, Windo fault, Kaindi fault, Demba fault.
- Fault's trending north-south includes Rara faults, Landai faults, and Lainea faults.

II. MATERIAL AND METHOD

The location of the research is precisely located in Lainea Village, where most of it is Lainea District, Morphotectonic analysis in watersheds was carried out in 9 (nine) watersheds scattered in the research area (Fig. 2). This research activity was carried out using two methods. The first method uses remote sensing by interpreting topographic maps at a scale of 1: 25,000 and satellite imagery maps of the Shuttle Radar Topography Mission-Digital Elevation Model (SRTM-DEM) with 0.27-arcsecond spatial resolution and EGM2008 vertical datum. The second method uses direct field observations to observe geological features formed due to faults and observe geological structures and the distribution of geothermal manifestations in the field.

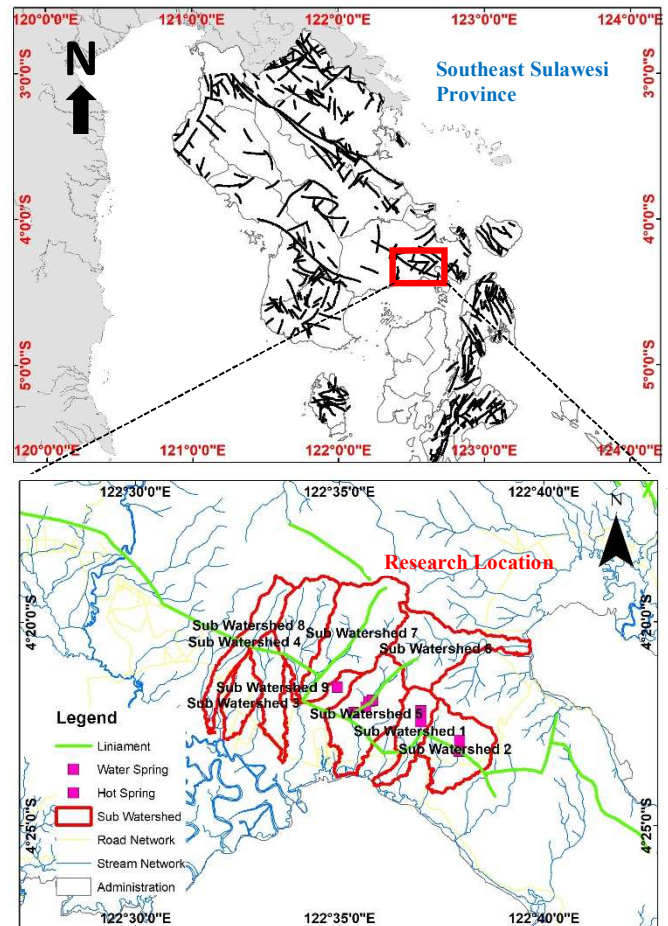


Fig. 2 Distribution of 9 (nine) sub-watersheds in research areas

The relationship between geomorphological features and tectonic activity that occurs is called morphotectonic analysis, where in this research activity, it is analyzed by 2 (two) types of parameters, namely: morphotectonic watershed (DAS), including hypsometric curves and hypsometric integrals (Hc

and H_i), stream length-gradient index (SL), Index of drainage basin shape (Bs), the ratio of valley floor width to valley height (Vf), and morphotectonics of Non-watersheds (Non-DAS) Index of mountain front sinuosity (Smf) (Table I). After processing the data using morphotectonic parameters, the analysis was carried out using the tectonic activity level classification (Table II) and the tectonic activity index relative (Table III).

TABLE I
MORPHOTECTONIC ANALYSIS PARAMETERS IN THE RESEARCH AREA

No.	Parameter	Equation	Source
1	Hypsometric Curves and Integral (H_i)	$H_i = \frac{(h_{\text{mean}} - h_{\text{min}})}{(h_{\text{max}} - h_{\text{min}})}$	[17], [18], [21]–[23]
2	Stream length-gradient index (SL)	$SL = \left(\frac{\Delta H}{\Delta L}\right) \times L$	[17], [18], [23]–[26]
3	Index of drainage basin shape (Bs)	$Bs = \frac{Bl}{Bw}$	[23], [27]
4	The ratio of valley floor width to valley height (Vf)	$Vf = \frac{2V_{fw}}{(E_{ld} - E_{sc}) + (E_{rd} - E_{sc})}$	[9], [17], [18], [23]
5	Index of mountain front sinuosity	$S_{mf} = L_{mf}/L_s$	[12], [17], [18], [23], [24]

TABLE II
TECTONIC ACTIVITY LEVEL USING MORPHOTECTONIC PARAMETERS [13], [15]

No.	Morphotectonic Parameters	Tectonic Activity Level		
		Class 1	Grade 2	Grade 3
1.	H_i	$(H_i \geq 0.5)$	$(0.4 \leq H_i < 0.5)$	$(H_i < 0.4)$
2.	SL	$(SL \geq 500)$	$(300 \leq SL < 500)$	$(SL < 300)$
3.	BS	$(Bs \geq 4)$	$(3 \leq Bs < 4)$	$(Bs \leq 3)$
4.	Vf	$(Vf < 0.3)$	$(0.3 < Vf < 1.0)$	$(Vf > 1.0)$
5.	Smf	$(Smf < 1.1)$	$(1.1 \leq Smf < 1.5)$	$Smf \geq 1.5$

TABLE III
TECTONIC ACTIVITY INDEX RELATIVE (iatr) [13], [15]

Tectonic Activity	Relative Tectonic Activity Index (IATR)
1	$1 \leq IATR < 1.5$
2	$1.5 \leq IATR < 2$
3	$2 \leq IATR < 2.5$
4	$IATR > 2.5$

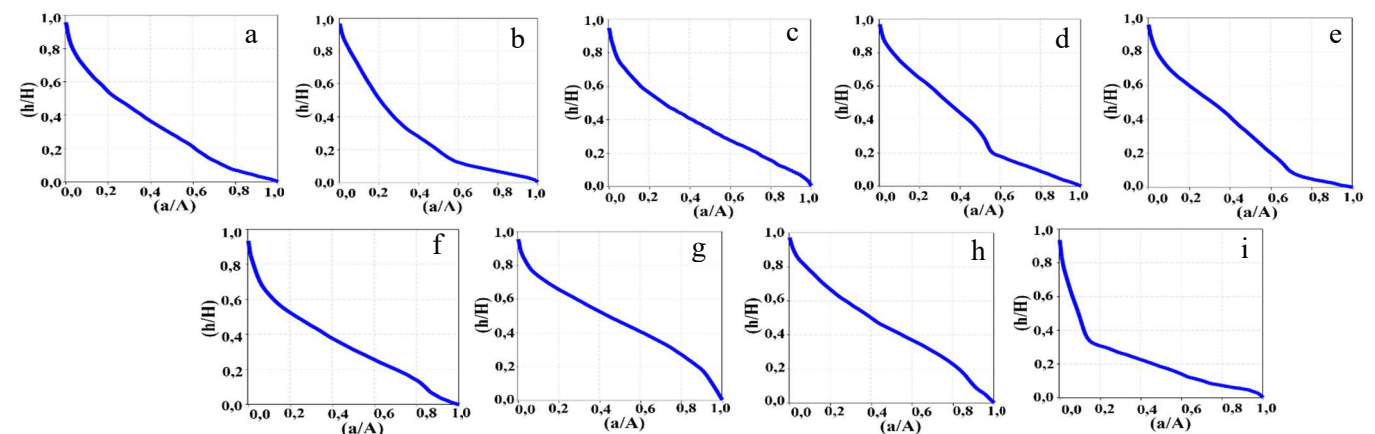


Fig. 3 (a) Hypsometric curve for sub-watershed 1, (b). The hypsometric curve for sub-watershed 2, (c). the hypsometric curve for sub-watershed 3, (d). the hypsometric curve for sub-watershed 4, (e). Hypsometric curve sub-watershed 5, (f). Hypsometric curve sub-watershed 6, (g). Hypsometric curve sub-watershed 8, (h). Hypsometric curve sub-watershed 8, (i). Hypsometric curve sub-watershed 9.

If the stage of an area is getting older, the shape of the curve will be more concave, where the point of curvature of the

III. RESULT AND DISCUSSION

A. Results of Sub-Watershed Morphotectonic Analysis

Hypsometric curves describe the transverse elevation distribution of a watershed or sub-watershed. The hypsometric curve is made by plotting on the Y-axis by entering the comparison value of the river basin height point (h/H) and on the X-axis using the watershed area value (a/A). In this research activity, the making of hypsometric curves was carried out in 9 (nine) sub-watersheds in the study area. The shape and pattern of the hypsometric curve resulting from the tectonic class analysis are quantitative. The H_i value can be divided into 3 tectonic classes, namely class 1 ($H_i \geq 0.5$), class 2 ($0.4 \leq H_i \leq 0.5$), class 3 ($H_i < 0.4$) [13], [15]. Also, the results of the calculation and depiction of the shape of the hypsometric curve show the morphological stage of an area, including the young stage, mature stage, and old stage.

Based on the results of data processing and analysis of the shape of the hypsometric curve of the study area, which shows 3 (three) classes of regional morphological stadia, namely young stage, mature stage, and old stage (see Fig. 3). The young stage area is in the sub-watershed 7, where the resulting hypsometric curve has an X-axis and a Y-axis above the diagonal line's midpoint ($X, Y > 0.5$). the shape of the hypsometric curve like this indicates that the tectonic process that occurs is more dominant than the erosion process that works, resulting in a rougher form of topographic relief in sub-watershed 7.

The mature stage area is in Sub-watershed 1, 2, 4, 5, 6, 8 where the resulting hypsometric curve approaches or passes through the X, Y axes at the center of the diagonal line ($X = Y = 0.5$). Also, the shape of a curve like this shows changes in the X and Y value that are almost proportional so that the curve formed approaches the diagonal line. The shape of the hypsometric curve like this indicates the tectonic process and the erosion process that occurs has the same effect. The old stage area is in sub-watersheds 3 and 9, where the resulting hypsometric curve is increasingly concave downward with decreasing value changes on the X and Y axes.

curve will be away from the diagonal line, and vice versa tends to get closer to 0. The shape of a curve like this indicates

that the erosion process is more dominant than the tectonic process. This resulted in a relatively flatter morphological form of the sub-watershed. Based on the analysis and processing of integral hypsometric data in 9 (nine) sub-watersheds in the study area, 3 (three) tectonic classes were produced, namely class 1, class 2, and class 3 (see Table IV).

The class 1 tectonic group with an integral hypsometric value (H_i) = 0.518 was found in the sub-watershed 7. Types of rock in sub-watershed 7 are slate, phyllite, and quartzite. Class 2 tectonic groups are found in sub-watersheds 1, 2, 4, 5, 6, and 8 with an integral hypsometric value (H_i) that varies between 0.404 to 0.464. the rock types that make up the area with class 2 tectonic groups are metamorphic rock units (consisting of phyllite and quartzite), meta-sandstone rock units, conglomerate rock units, and alluvium. Class 3 tectonic groups are found in sub-watersheds 3 and 9 where the integral hypsometric value (H_i) is 0.259 and 0.273. the rock types that make up the area with tectonic class 3 are in the form of conglomerate and alluvium rock units. The distribution of tectonic classes in the study area can be seen in Fig. 4, where the red color is a symbol of class 1 tectonic class, the yellow tectonic class 2, and the green tectonic class 3.

TABLE IV
RESULTS OF INTEGRAL HYPSONETRIC CALCULATION

Sub-Watershed	Maximum Elevation (m)	Minimum Elevation (m)	Average Elevation (m)	H_i	Tectonic Class
1	437.5	12.5	203.6	0.450	2
2	400	12.5	169.2	0.404	2
3	112.5	12.5	39.8	0.273	3
4	512.5	12.5	230	0.435	2
5	400	12.5	174.7	0.407	2
6	462.5	12.5	221.4	0.464	2
7	512.5	12.5	289.8	0.518	1
8	437.5	12.5	203.6	0.449	2
9	300	12.5	87.2	0.259	3

The stream length gradient index (SL) analysis was carried out in 9 sub-watershed areas by plotting the location points of as many as 166 points scattered in the villages of Kaindi, Lainea, Pamandati, and Pangan Jaya. Then, from the analysis results in each sub-watershed, the highest SL value was taken as the basis for determining the tectonic class of the research area (Fig. 5). Based on the analysis of the stream length gradient index value (SL), it is produced that the tectonic class of the study area is divided into 3 classes, namely, class 1 ($SL \geq 500$), class 2 ($300 \leq SL < 500$), and class 3 ($SL < 300$) [13], [15], with a range of SL values obtained from 2,560 to 561,213.

The result of SL analysis in sub-watershed 1 obtained a range of values starting from 21,199-231,156 which indicates tectonics class 3, sub-watershed 2 obtained a range of SL values starting from 41,355-194,775 which indicates tectonic class 3, sub watershed3 obtained a range SL values start from 19,919-43,034 which indicates tectonic class 3, sub-watershed 4 it is obtained that the range of SL values starts from 14,074-561,213 which indicates tectonic class 1, sub-watershed 5 obtained a range of SL values starting from 38,645-277,356 where this value indicates tectonic class 3, sub-watershed 6 obtained a range of SL values starting from 2,559-140,131 which indicates tectonic class 3, sub-watershed 7 obtained a range of SL values starting from 18,778-486,573 which indicates tectonic class 2, sub-

watershed 8 obtained a range of SL values starting from 46,363-418,913 which indicates tectonic class 2, and sub-watershed 9, it is obtained that the range of SL values starts from 38,556-101,013 which indicates tectonic class 3.

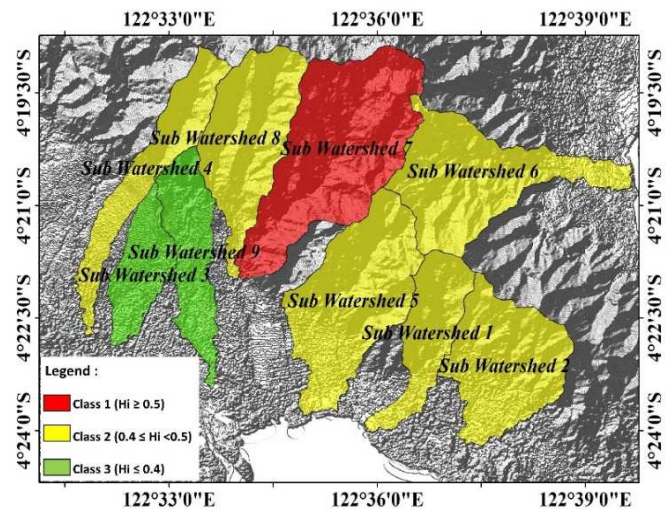


Fig. 4 The distribution of tectonic classes based on Integral Hypsometric values in the study area.

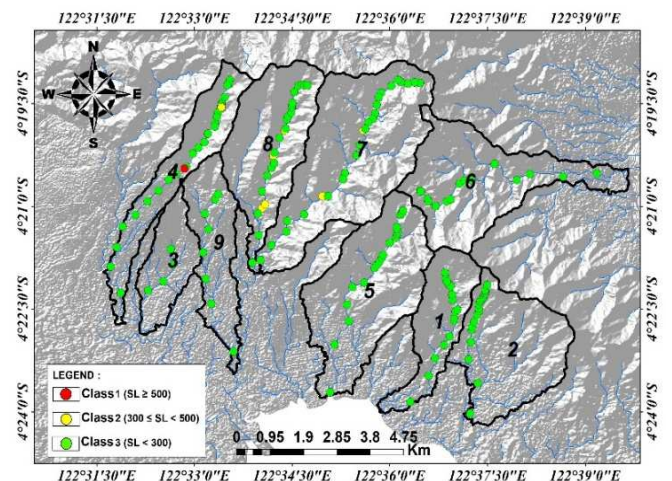


Fig. 5 Distribution map of the results of the SL value analysis in the study area

The basin shape index analysis is calculated using the comparison value between the basin length (BL) and the basin width. The value of B_s can describe the level of tectonic activity [15]. In areas with active tectonics, it will form a watershed with an elongated shape, while in less active areas, the shape of the watershed will be rounded. The division of tectonic classes based on the value of B_s is divided into three classes, namely class 1 ($B_s \geq 4$), class 2 ($3 \leq B_s < 4$), and class 3 ($B_s \leq 3$) [13], [15].

The value of B_s was calculated in 9 (nine) sub-watersheds were the results of the B_s value ranged from 1,237 to 5,783. The details of the B_s value of each sub-watershed are as follows:

- Sub-watershed 1 obtained a B_s value of 3,029 and is classified as tectonic class 2 with the shape of the watershed tends to be elongated.
- Sub-watershed 2 obtained a B_s value of 1,237 and is classified as tectonic class 3 with the shape of the watershed tends to be rounded.

- Sub-watershed 3 obtained a Bs value of 3,019 classified as tectonic class 2, with a watershed shape that tends to be elongated.
- Sub-watershed 4 obtained a Bs value of 5,783 classified as tectonic class 1 with an elongated watershed.
- Sub-watershed 5 obtained a Bs value of 2,092 classified as tectonic class 3 with a watershed shape that tends to be rounded.
- Sub-watershed 6 obtained a Bs value of 1,836 classified as tectonic class 3 with a watershed shape that tends to be rounded.
- Sub-watershed 7 obtained a Bs value of 2,059 classified as tectonic class 3 with the shape of the watershed, which tends to be rounded.
- Sub-watershed 8 obtained a Bs value of 2,312 classified as a tectonic class of the sub-watershed tends to be rounded.
- Sub-watershed 9 obtained a Bs value of 4,018 and is classified as tectonic class 1 with an elongated watershed shape (see Table V)

Based on the results of the analysis of the watershed shape index, it can be concluded that a high value of Bs will indicate the elongation of the river basin (elongated basins), while a low value of Bs indicates a circular basin, the distribution of the results of the analysis of Bs can be seen on Fig. 6.

TABLE V
THE RESULTS OF CALCULATING THE VALUE OF BS IN 9 (NINE) SUB-WATERSHEDS

Sub-Watershed	Bl	Bw	Bs	Tectonic Class
1	4,623,852	1,526,053	3,029	2
2	4,239,799	3,427,835	1,237	3
3	4,318,055	1,430,045	3,019	2
4	6,900,224	1,193,146	5,783	1
5	5,991,785	2,863,656	2,092	3
6	6,623,865	3,607,315	1,836	3
7	7,178,896	3,486,620	2,059	3
8	5,617,276	2,429,429	2,312	3
9	5,901,630	1,468,638	4,018	1

The calculation of the Vf value is carried out in 7 (seven) sub-watersheds in the study area, which is done by drawing 13 (thirteen) lines which will then be calculated by comparing the width of the valley with the elevation of the hills that flank it. The division of tectonic classes based on the Vf value is divided into three classes, namely class 1 ($Vf < 0.3$), class 2 ($0.3 < Vf < 1.0$), and class 3 ($Vf \geq 1.0$) [13], [15]. From the results of the calculation of the Vf value in the study area, it is found that the Vf value ranges from 0.121 to 0.815.

The results of the calculation of the Vf value obtained in the 7 (seven) sub-watersheds are as follows: (TABLE VI).

- Sub-watershed 1 was drawn 2 Vf lines and obtained Vf values of 0.303 and 0.381, where these values are classified in tectonic class 2.
- Sub-watershed 2 is drawn 1 Vf line and the results are a Vf value of 0.815 which is classified into tectonic class 2.
- Sub-watershed 4 carried out 2 draws of Vf lines and obtained Vf values of 0.419 and 0.541 where these values are categorized in tectonic class 2.
- Sub-watershed 5 carried out 2 draws of the Vf line with the results of the calculation, namely 0.344 and 0.497 where these values are classified in the tectonic class 2.

- Sub-watershed 6, 1 drawing of the Vf line is carried out with the calculation result of 0.401 where this value is classified in the tectonic class 2.
- Sub-watershed 7 was drawn 2 Vf lines and obtained values of 0.165 and 0.121 where these values are classified in tectonic class 1.
- Sub-watershed 8 was drawn 2 Vf lines and obtained values of 0.346 and 0.635 where these values are classified into tectonic class 2.

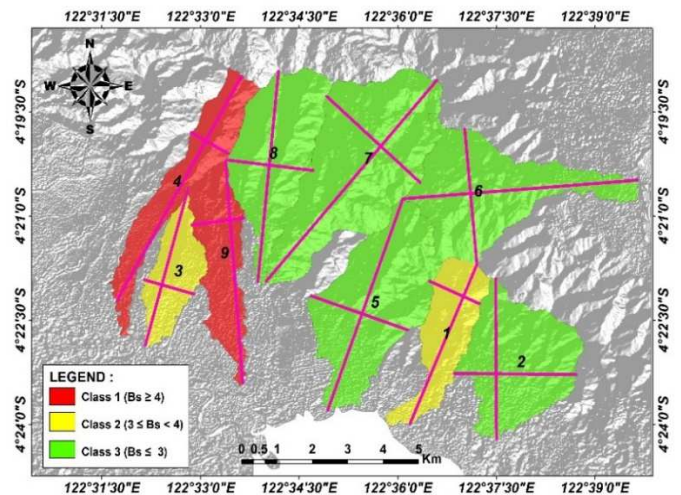


Fig. 6 The distribution of the analysis results of the watershed index (Bs) in the study area.

The value of Vf or the width of the valley floor has an important meaning to the geological process that occurs, where when the resulting Vf value has a high value, it will be associated with a low level of lift velocity. Meanwhile, for low Vf values indicate the shape of a deep river valley so that it can be associated with the lifting activity that occurs is quite high.

The results of direct observations in the field on the river valley that is formed show that the river valley in the form of "V" produces a low Vf value, thus indicating an active lift, while in the river valley "U" produces a high Vf value so that it can indicate the formation of a result. high lateral erosive activity (see **Error! Reference source not found.**).

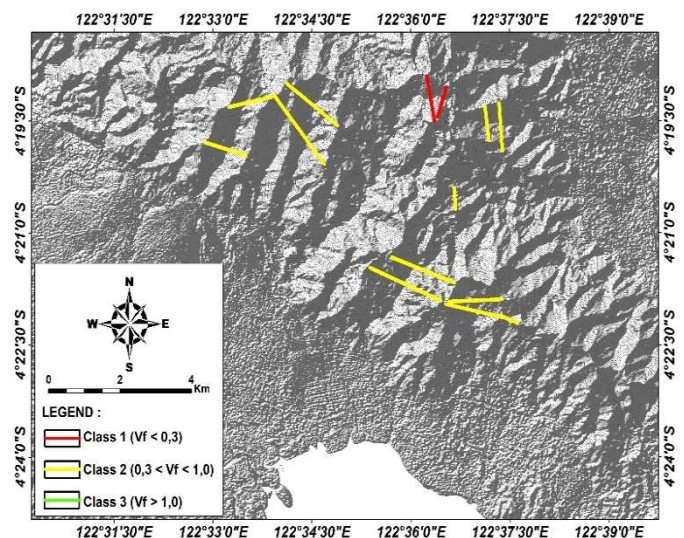


Fig. 7 Map of distribution of Vf value calculation

The value of Vf in the research area resulting from data processing shows a steep and narrow shape so that it can be grouped into medium (class 2) to high (class 1) tectonic activity levels. Index of mountain front sinuosity (Smf) is a value that reflects the balance between the causes/forces of erosion that tend to cut along the front of the mountains to form indentations and tectonic forces/ forces that directly produce mountain faces and correspond to the active fault zone that reflects active tectonics. Low Smf values are associated with active tectonics and uplifting directly. If the speed decreases, the erosion process will occur and erode the mountain's faces irregularly, and the Smf value will be higher. The tectonic class based on the Smf value is divided into 3, namely, tectonic class 1 ($Smf < 1,1$), tectonic class 2 ($1,1 \leq Smf < 1,5$), and tectonic class 3 ($Smf \geq 1,5$) [13], [15]

TABLE VI
THE RESULTS OF THE CALCULATION OF THE VALUE OF Vf

DAS	No.	Vfw	Eld	Erd	Esc	Vf
DAS 1	1	50	362.5	387.5	210	0.303
	2	70	325	362.5	160	0.381
DAS 2	1	55	325	350	270	0.815
	2	65	325	375	195	0.419
DAS 4	1	75	437.5	500	330	0.541
	2	65	325	375	195	0.419
DAS 5	1	100	287.5	375	130	0.497
	2	70	325	362.5	140	0.343
DAS 6	1	34	237.5	262.5	165	0.4
	2	20	475	475	310	0.121
DAS 7	1	20	437.5	475	335	0.165
	2	20	475	475	310	0.121
DAS 8	1	150	400	512.5	220	0.635
	2	70	487.5	537.5	310	0.346

The calculation of Smf was not carried out in all locations in the study area but only in the mountainous face zone or the transitional /transition zone between the mountain topography and the plain. The results of the Smf value calculation ranged from 1.086 to 2.585, where at location 1 the results of the calculation of the Smf value obtained were 1.094, which indicated the tectonic class 1. The results of the Smf value calculation at location 2, the value obtained was 1.086, which indicates the tectonic class 1. The results of the calculation of the value Smf at location 3 the value obtained is 1.097, where this value is included in the tectonic class classification 1. The results of the calculation of Smf at location 4 obtained an Smf value of 1.370, which indicates the tectonic class 2. The results of calculating the value of Smf at location 5 obtained a value of 1.344, where this value indicates tectonic class 2.

TABLE VII
RESULTS OF THE CALCULATION OF THE VALUE OF SMF

No.	Lmf	Ls	Smf	Tectonic Class
1	2,252.4	2,058.5	1,094	1
2	2,497.2	2,299.4	1,086	1
3	2,528.7	2,304.5	1,097	1
4	3,290.5	2,401.5	1,370	2
5	3,131.8	2,330.7	1,343	2
6	2,310.4	1,490.6	1.55	3
7	4,476.9	2,722.9	1,644	3
8	6,545.5	2,531.9	2,585	3

In general, the results of the calculation of the Smf value in the study area consist of tectonic class 1, tectonic class 2, and tectonic class 3, where tectonic class 2 shows the balance between the tectonic process and the ongoing erosion process, and tectonic class 3 shows the tectonic process is slowing down so that what happens is the more dominant erosion process occurs (see Fig. 8 and Tables VII).

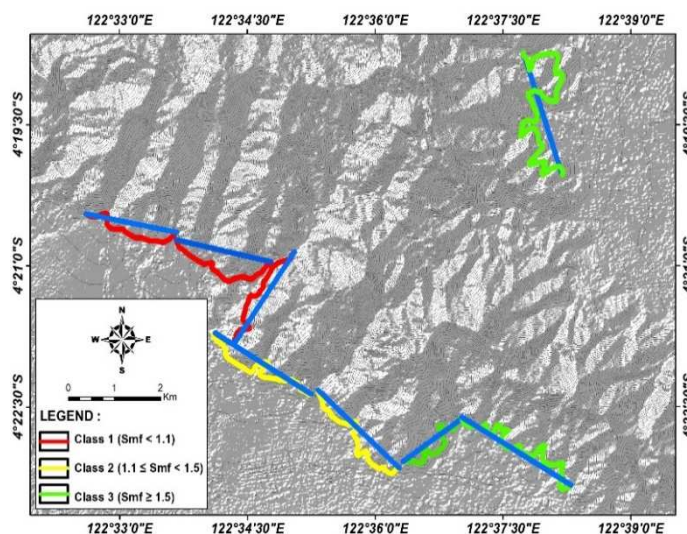


Fig. 8 Map of distribution of Smf in the study area

There are 5 (five) morphometric parameters used in the calculation of the tectonic class relative to the 9 (nine) sub-watersheds in the study area. Overlay analysis in determining relative tectonic activity is carried out by taking 5 (five) watershed morphometric parameters, namely hypsometric curves and hypsometric integrals, river length gradient index (SL), watershed shape index (Bs), and valley floor ratio (Vf), as well as non-watershed morphometry, namely mountain front sinuosity (Smf).

Furthermore, each morphometric parameter is added according to its class, and the relative tectonic activity index value is made, and the tectonic activity class is divided based on the IATR value of the five morphometric parameters. The tectonic activity class based on the average value or IATR is divided into four classes [13], [15], namely:

- Very high tectonic activity class ($1 \leq IATR < 1.5$)
- High tectonic activity class ($1.5 \leq IATR < 2$)
- Medium tectonic activity class ($2 \leq IATR < 2.5$)
- Low tectonic activity class ($IATR \geq 2.5$)

So that based on this classification, the results of the calculation of the relative tectonic activity index value are described in Fig. 9 and Table VIII)

TABLE VIII
IATR VALUE CALCULATION RESULTS

Sub-Watershed	HI	Bs	SL	Vf	Smf	IATR
1	2	2	3	2	3	2,4
2	2	3	3	2	3	2,6
3	3	2	3			2,67
4	2	1	1	2	1	1,4
5	2	3	3	2	2	2,4
6	2	3	3	2		2,5
7	1	3	2	1	1	1,6
8	2	3	2	2	1	2
9	3	1	3		1	2

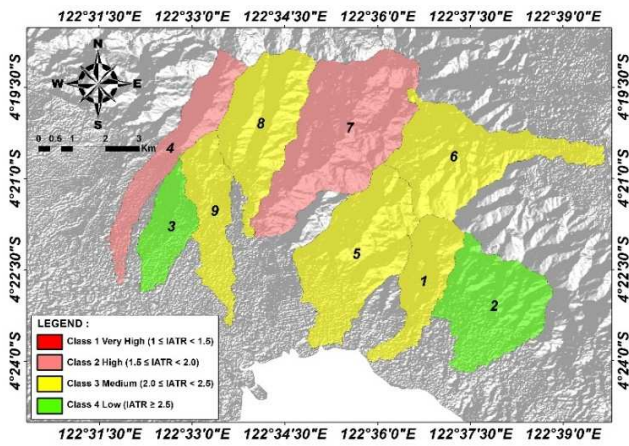


Fig. 9 Map of distribution of IATR calculation results

The results of calculations and analysis show that not all four classes of tectonic activity are in the study area. The tectonic activity classes are only class 2 (high), class 3 (medium), and class 4 (low). A high tectonic class is found in sub-watershed 4 with an IATR value of 1.4 and sub-watershed 7 with an IATR value of 1.6. A medium tectonic class is found in sub-watershed 1 with an IATR value of 2.4, sub-river basin 5 with an IATR value of 2.4, sub-watershed 6 with an IATR value of 2.5, sub-watershed 8 with a value IATR 2, and sub-watershed 9 with IATR value 2. Furthermore, the low tectonic class is in sub-watershed 2 with an IATR value of 2.6 and sub-river basin 3 with an IATR value of 2.67.

B. Field Observation Results

The geological structure in the study area is directly observed and measured in the field. Geological structure data were taken in the form of joints and folds. The measurements carried out in the study area obtained a joint spread across two villages, namely Lainea Village and Pamandati Village.

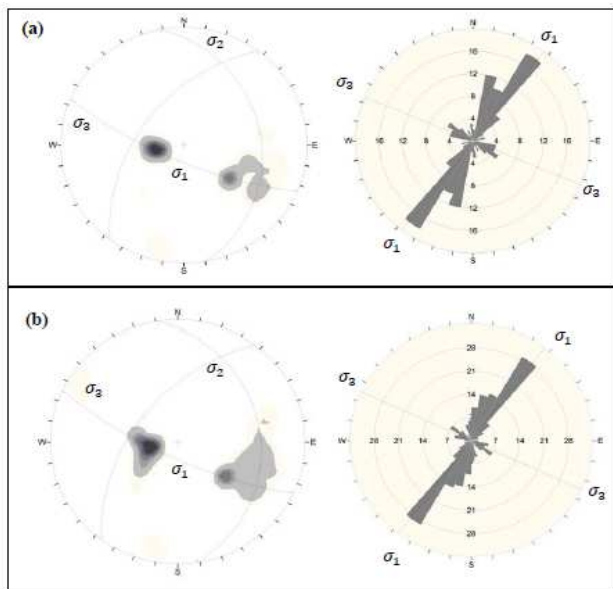


Fig. 10 (a) Stereonet and roset diagram of the strength measurement data in the rocks of Lainea area, (b) Rosset diagram on the statistical measurement of the Pamandati area.

Based on the results of the measurement of the joint data in the Lainea Village area, which was then processed using dips

software, the dominant direction was Northeast-Southwest, while in the Pamandati area the dominant direction was Northeast-Southwest, these two muscular dominant directions correspond to the direction of formation of the Boro-Boro fault that develops in the study area (see Fig. 10).

Geological structure data contained in the study area is also supported by the presence of hot springs scattered in Lainea, Pamandati, and Kaindi Villages, en echelon vein and the presence of fault brecciation zones in Lainea Village with the direction of N201°E and the one is in Pangan Jaya Village with the direction N195°E (see Fig. 11).



Fig. 11 (a). Fault brecciation zone in Lainea Village, (b). Fault brecciation zone in Pangan Jaya, (c). En echelon vein in meta-sediment rocks, (d). Hot water pool in Pamandati Village, (e). Hot springs in Kaindi Village, (f). Hot springs in Lainea Village.

Other traces of geological structures other than burly are visible in the form of folds that occur in meta-sedimentary rock, the span length of the fold is estimated to be 17.5 meters. (Fig. 12). The type of folds found is a complex of folds consisting of anticline and syncline folds; after reconstruction, the actual model of these folds was found (Fig. 13)



Fig. 12 Geological traces are found in the form of folds in the rock.

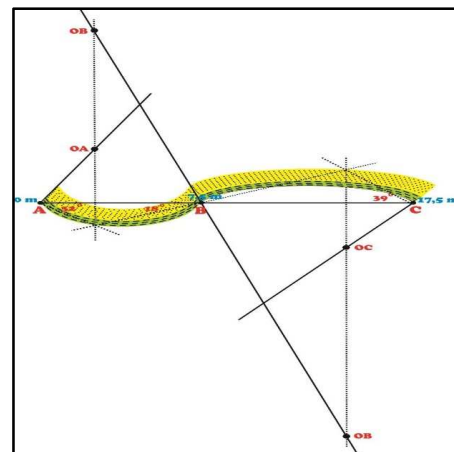


Fig. 13 The results of fold reconstruction in Pamandati Village

IV. CONCLUSION

Based on the results of the morphometric analysis of the sub-watersheds in the study area, it can be concluded that the level of tectonic activity in the study area can be grouped into 3 (three) classes, including: 1) high tectonic activity class in sub-watersheds 4 and 7, 2) medium tectonic activity classes in sub-watersheds 1, 5, 6, 8, 9, and 3) low tectonic activity classes in sub-watersheds 2 and 3. Based on the results of the research that has been carried out, it is very important to identify the level of tectonic activity based on the aspects of the earthquake that occurred as well as the potential magnitude of the earthquake that will occur due to the movement of several segments of the geological structure in the study area.

ACKNOWLEDGMENT

We thank Halu Oleo University for assisting, especially funding assistance, in the Leading Higher Education Internal Basic Research program of the 2020.

REFERENCES

- [1] A. Maulana, M. Bröcker, and W. Dan, "Petrogenesis and geochronology of Cenozoic intrusions in the Poboya and Sassak gold and copper districts in Western Sulawesi, Indonesia: Implications for the mineralization processes and magma sources," *Journal of Asian Earth Sciences*, vol. 193, p. 104303, May 2020, doi: 10.1016/j.jseae.2020.104303.
- [2] A. Maulana, K. Watanabe, and K. Yonezu, "IJEScA Petrology and Geochemistry of Granitoid from South Sulawesi, Indonesia: Implication for Rare Earth Element (REE) Occurrences," *International Journal of Engineering and Science Applications*, vol. 3, no. 1, pp. 79–86, Jul. 2016.
- [3] I. M. Watkinson and R. Hall, "Fault systems of the eastern Indonesian triple junction: evaluation of Quaternary activity and implications for seismic hazards," *Geological Society, London, Special Publications*, vol. 441, no. 1, pp. 71 LP–120, Jan. 2017, doi: 10.1144/SP441.8.
- [4] X. Zhang *et al.*, "A Late Miocene magmatic flare-up in West Sulawesi triggered by Banda slab rollback," *GSA Bulletin*, vol. 132, no. 11–12, pp. 2517–2528, Nov. 2020, doi: 10.1130/b35534.1.
- [5] L. Sarmili, "Opening Structure of the Bone Basin on South Sulawesi in Relation to Process of Sedimentation," *Bulletin of the Marine Geology*, vol. 30, no. 2, p. 97, Feb. 2016, doi: 10.32693/bomg.30.2.2015.79.
- [6] A. M. S. Nugraha and R. Hall, "Late Cenozoic palaeogeography of Sulawesi, Indonesia," *Palaeogeography, Palaeoclimatology, Palaeoecology*, vol. 490, pp. 191–209, 2018, doi: <https://doi.org/10.1016/j.palaeo.2017.10.033>.
- [7] L. T. White, R. Hall, and R. A. Armstrong, "The age of undeformed dacite intrusions within the Kolaka Fault zone, SE Sulawesi, Indonesia," *Journal of Asian Earth Sciences*, vol. 94, pp. 105–112, Aug. 2014, doi: 10.1016/j.jseae.2014.08.014.
- [8] Z. Wu and M. Hu, "Neotectonics, active tectonics and earthquake geology: terminology, applications and advances," *Journal of Geodynamics*, vol. 127, pp. 1–15, 2019, doi: <https://doi.org/10.1016/j.jog.2019.01.007>.
- [9] D. Gentana, N. Sulaksana, E. Sukiyah, and E. T. Yuningsih, "Index of active tectonic assessment: Quantitative-based geomorphometric and morphotectonic analysis at Way Belu Drainage Basin, Lampung Province, Indonesia," *International Journal on Advanced Science, Engineering and Information Technology*, vol. 8, no. 6, pp. 2460–2471, Dec. 2018, doi: 10.18517/ijaseit.8.6.6089.
- [10] G. I. Marliyani, J. R. Arrowsmith, and K. X. Whipple, "Characterization of slow slip rate faults in humid areas: Cimandiri fault zone, Indonesia," *Journal of Geophysical Research: Earth Surface*, vol. 121, no. 12, pp. 2287–2308, Dec. 2016, doi: <https://doi.org/10.1002/2016JF003846>.
- [11] D. M. Maurya, V. Chowksey, P. Tiwari, and L. S. Chamyal, "Tectonic geomorphology and neotectonic setting of the seismically active South Wagad Fault (SWF), Western India, using field and GPR data," *Acta Geophysica*, vol. 65, no. 6, pp. 1167–1184, 2017, doi: 10.1007/s11600-017-0099-5.
- [12] D. Gentana, N. Sulaksana, E. Sukiyah, and E. T. Yuningsih, "Morphotectonics of mount rendingan area related to the appearances of geothermal surface manifestations," *Indonesian Journal on Geoscience*, vol. 6, no. 3, pp. 291–309, Dec. 2019, doi: 10.17014/ijog.6.3.291-309.
- [13] R. El Hamdouni, C. Irigaray, T. Fernández, J. Chacón, and E. A. Keller, "Assessment of relative active tectonics, southwest border of the Sierra Nevada (southern Spain)," *Geomorphology*, vol. 96, no. 1–2, pp. 150–173, Apr. 2008, doi: 10.1016/j.geomorph.2007.08.004.
- [14] S. Topal, "Quantitative analysis of relative tectonic activity in the Acıgöl fault, SW Turkey," *Arabian Journal of Geosciences*, vol. 11, no. 9, p. 198, 2018, doi: 10.1007/s12517-018-3545-z.
- [15] M. Dehbozorgi, M. Pourkermani, M. Arian, A. A. Matkan, H. Motamedi, and A. Hosseiniasl, "Quantitative analysis of relative tectonic activity in the Sarvestan area, central Zagros, Iran," *Geomorphology*, vol. 121, no. 3–4, pp. 329–341, Sep. 2010, doi: 10.1016/j.geomorph.2010.05.002.
- [16] S. Supartoyo, C. Sulaiman, and D. Junaedi, "Kelas tektonik sesar Palu Koro, Sulawesi Tengah," Aug. 2014.
- [17] M. Softa, T. Emre, H. Sözbilir, J. Q. G. Spencer, and M. Turan, "Geomorphic evidence for active tectonic deformation in the coastal part of Eastern Black Sea, Eastern Pontides, Turkey," *Geodinamica Acta*, vol. 30, no. 1, pp. 249–264, Jan. 2018, doi: 10.1080/09853111.2018.1494776.
- [18] A. A. Wani, B. S. Bali, and S. Lone, "Drainage Characteristics of Tectonically Active Area: An Example from Mawar Basin, Jammu and Kashmir, India," *Journal of the Geological Society of India*, vol. 93, no. 3, pp. 313–320, Mar. 2019, doi: 10.1007/s12594-019-1179-8.
- [19] A. Zarkasyi and S. Widodo, "Survei Magnetotellurik (MT) dan Time Domain Electro Magnetic (TDEM) Daerah Panas Bumi Lainea, Provinsi Sulawesi Tenggara," May 2015, doi: 10.5281/ZENODO.2529113.
- [20] S. Hadi, Nur; Suwarno; Limar, Kencanaawati; Dede, Dinarsih; Ria, "Laporan Akhir Penyelidikan Terpadu Geologi dan Geokimia Daerah Panas Bumi Lainea," *Pusat Sumberdaya Geologi, Badan Geologi*, 2010. [Online]. Available: <http://psdg.bgl.esdm.go.id/perpus/alihmedia/LS20104PB/>. [Accessed: 06-Dec-2020].
- [21] T. Zhang, S. Fan, S. Chen, S. Li, and Y. Lu, "Geomorphic Evolution and Neotectonics of the Qianhe River Basin on the Southwest Margin of the Ordos Block, North China," *Journal of Asian Earth Sciences*, vol. 176, pp. 184–195, 2019, doi: <https://doi.org/10.1016/j.jseae.2019.02.020>.
- [22] R. Ahmed, H. Sajjad, and I. Husain, "Morphometric Parameters-Based Prioritization of Sub-watersheds Using Fuzzy Analytical Hierarchy Process: A Case Study of Lower Barpani Watershed, India," *Natural Resources Research*, vol. 27, no. 1, pp. 67–75, Jan. 2018, doi: 10.1007/s11053-017-9337-4.
- [23] A. K. Anand and S. P. Pradhan, "Assessment of Active Tectonics from Geomorphic Indices and Morphometric Parameters in Part of Ganga basin," *Journal of Mountain Science*, vol. 16, no. 8, pp. 1943–1961, 2019, doi: 10.1007/s11629-018-5172-2.
- [24] E. A. Keller and N. Pinter, *Active Tectonics: Earthquakes, Uplift, and Landscape*, 2nd Editio. New Jersey: Prentice Hall, 2002.
- [25] A. Moussi, N. Rebaï, A. Chaieb, and A. Saâdi, "GIS-Based Analysis of the Stream Length-Gradient Index for Evaluating Effects of Active Tectonics: a Case Study of Enfidha (North-East of Tunisia)," *Arabian Journal of Geosciences*, vol. 11, no. 6, p. 123, 2018, doi: 10.1007/s12517-018-3466-x.
- [26] S. Das and K. Gupta, "Morphotectonic Analysis of the Sali River Basin, Bankura District, West Bengal," *Arabian Journal of Geosciences*, vol. 12, no. 7, p. 244, 2019, doi: 10.1007/s12517-019-4406-0.
- [27] C. He *et al.*, "Geomorphological signatures of the evolution of active normal faults along the Langshan Mountains, North China," *Geodinamica Acta*, vol. 30, no. 1, pp. 163–182, Jan. 2018, doi: 10.1080/09853111.2018.1458935.